

# Conjugated Polymer with Ternary Electron-Deficient Units for Ambipolar Nanowire Field-Effect Transistors

Yunjing Ji,<sup>1,2†</sup> Chengyi Xiao,<sup>1†</sup> Gaël H. L. Heintges,<sup>3</sup> Yonggang Wu,<sup>2</sup> René A. J. Janssen,<sup>3</sup> Deqing Zhang,<sup>1</sup> Wenping Hu,<sup>1</sup> Zhaohui Wang,<sup>1</sup> Weiwei Li<sup>1</sup>

<sup>1</sup>Beijing National Laboratory for Molecular Sciences, CAS Key Laboratory of Organic Solids, Institute of Chemistry, Chinese Academy of Sciences, Beijing 100190, People's Republic of China

<sup>2</sup>College of Chemistry and Environmental Science, Hebei University, Baoding 071002, China

<sup>3</sup>Molecular Materials and Nanosystems and Institute for Complex Molecular Systems, Eindhoven University of Technology, 5600 MB, Eindhoven, The Netherlands

Correspondence to: Y. Wu (E-mail: wuyonggang@hbu.edu.cn) or Z. Wang (E-mail: wangzhaohui@iccas.ac.cn) or W. Li (E-mail: liweiwei@iccas.ac.cn)

published online 00 Month 2015

DOI: 10.1002/pola.27898

**KEYWORDS:** conjugated polymers; crystallization; polymer nanowire; self-assembly

**INTRODUCTION** Organic field-effect transistors (OFETs) based on conjugated polymers have improved significantly in the last decade. Electron and hole mobilities above  $1 \text{ cm}^2 \text{ V}^{-1} \text{ s}^{-1}$  have been achieved,<sup>1–3</sup> exceeding those of amorphous silicon-based devices. Specifically, conjugated polymers capable of effectively transporting electrons and holes in single-component ambipolar OFETs<sup>4–6</sup> have been developed for application in CMOS-like circuits<sup>7</sup> and light-emitting transistors.<sup>8</sup> To realize ambipolar OFETs with stable hole and electron injection, the highest occupied molecular orbital (HOMO) level of the conjugated polymers should be close to  $-5.0 \text{ eV}$  for hole injection and the lowest unoccupied molecular orbital (LUMO) level close to or below  $-4.0 \text{ eV}$ .<sup>9</sup> Hence, a relatively small band gap is desirable, but such materials remain much less explored than polymers that are tuned to transport either holes or electrons.

Conjugated polymers that incorporate electron-donating units (D) and electron-withdrawing units (A) into the conjugated backbone have been extensively developed for organic electronics, in which absorption spectra and energy levels can be finely tuned via intra-molecular charge transfer.<sup>10</sup> The band gap can be lowered by introducing strong electron-rich and electron-deficient units.<sup>11</sup> Alternatively, conjugated polymers composed of mainly electron-deficient units are also known to attain small band gaps, with deep LUMO energy levels that are beneficial for electron injection. Several

acceptor-rich polymers with small band gaps have been reported for efficient n-type<sup>12–15</sup> and ambipolar OFETs.<sup>16–19</sup>

In this work, we selected three electron-deficient units, diketopyrrolopyrrole (DPP), benzothiadiazole (BT), and naphthalenediimide (NDI) to construct a small band gap polymer for ambipolar OFETs. Conjugated polymers based on electron-deficient DPP and BT have been reported to have balanced hole and electron mobilities in inert atmosphere,<sup>16</sup> but the LUMO level of  $-4.0 \text{ eV}$  precludes air-stable n-type transport. To further lower the LUMO level, NDI is considered as the third acceptor. NDI-based polymers have been reported to provide air-stable n-type charge transport because of the strong electron-withdrawing ability of NDI unit, resulting in deep LUMO levels.<sup>20</sup> However, it is difficult to observe p-type mobility in NDI-polymer FETs due to their deep HOMO levels.<sup>21</sup>

Therefore, it is interesting to explore a polymer consisting of all three acceptors and investigate its physical and electrical properties. The new regioregular polymer PDPP2T-BT-co-NDI (Fig. 1) is found to have an ultra-small band gap of  $1.21 \text{ eV}$ , deep LUMO level at  $-4.28 \text{ eV}$ , and a HOMO level at  $-5.49 \text{ eV}$ . The polymer is used to fabricate polymer nanowire FETs, which show high hole and electron mobility of  $1.61$  and  $0.98 \text{ cm}^2 \text{ V}^{-1} \text{ s}^{-1}$  respectively in inert atmosphere and  $1.64$  and  $0.14 \text{ cm}^2 \text{ V}^{-1} \text{ s}^{-1}$  in ambient air. These results demonstrate that the design strategy of incorporating multi-

Yunjing Ji and Chengyi Xiao contributed equally to this work.

Additional Supporting Information may be found in the online version of this article.

© 2015 Wiley Periodicals, Inc.

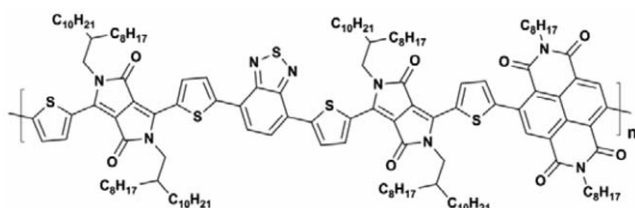


**FIGURE 1** The conjugated polymer PDPP2T-BT-*co*-NDI with ternary electron acceptors comprising DPP, BT, and NDI.

electron acceptors into one conjugated polymer is an effective method to finely tune the energy level for high performance ambipolar OFETs.

The regioregular PDPP2T-BT-*co*-NDI polymer was synthesized using the dibrominated extended monomer T-DPP-T-BT-T-DPP-T and the distannylated NDI monomer via Stille polymerization as is shown in the Supporting Information (Supporting Information Scheme S1). A solvent mixture of toluene/DMF (10:1, vol/vol) and a catalyst system based on  $\text{Pd}_2(\text{dba})_3/\text{PPh}_3/\text{CuI}$  was used to obtain high-molecular-weight polymers. We note that the polymerization reaction did not proceed when CuI was omitted. The molecular weight of the polymer was determined by gel permeation chromatography (GPC) using *o*-dichlorobenzene (*o*-DCB) as eluent. To reduce aggregation, the GPC column was kept at 140 °C and the polymer concentration was reduced to 0.1 mg mL<sup>-1</sup>. PDPP2T-BT-*co*-DTP possesses a very high molecular weight of  $M_n = 100.9 \text{ kg mol}^{-1}$  with polydispersity index of 2.75, comparable with other DPP polymers (Supporting Information Fig. S1).<sup>22</sup>

Solution and thin film UV-vis absorption spectra of PDPP2T-BT-*co*-NDI are shown in Figure 2. The polymer shows a red-shifted absorption in thin films with a slightly smaller optical band gap ( $E_g$ ) of 1.21 eV compared to that in chloroform

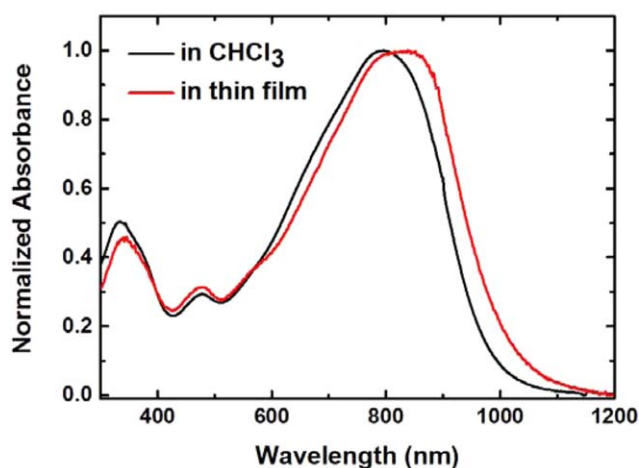


**FIGURE 2** UV-vis absorption spectra of PDPP2T-BT-*co*-NDI in  $\text{CHCl}_3$  solution (black line) and in solid-state films (red line). [Color figure can be viewed in the online issue, which is available at [wileyonlinelibrary.com](http://wileyonlinelibrary.com).]

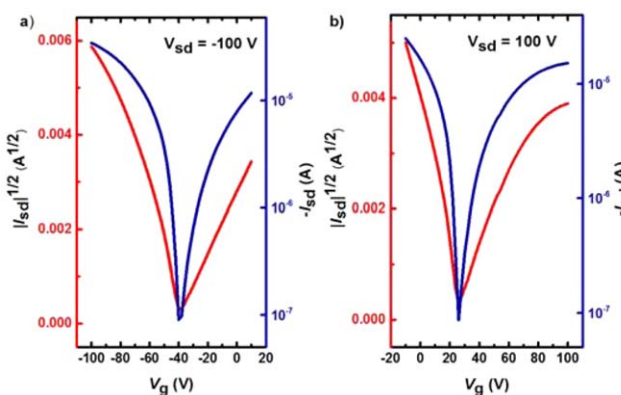


**FIGURE 3** (a) p-type and (b) n-type transfer characteristics for PDPP2T-BT-*co*-NDI thin films based OFETs at optimized annealing temperatures with bottom contact configuration measured under inert atmosphere. [Color figure can be viewed in the online issue, which is available at [wileyonlinelibrary.com](http://wileyonlinelibrary.com).]

solution ( $E_g = 1.25 \text{ eV}$ ), indicating aggregation. The optical band gap of PDPP2T-BT-*co*-NDI is similar to its analogous copolymers, PDPP-TBT<sup>19</sup> ( $E_g = 1.20 \text{ eV}$ ) and PNDI-DPP<sup>18</sup> ( $E_g = 1.15 \text{ eV}$ ).

Interestingly, introduction of the third electron-acceptor has a strong influence on the frontier orbital energy levels of the polymers.<sup>23</sup> The binary acceptor polymer PDPP-TBT (with DPP and BT units) has a LUMO energy of  $-4.01 \text{ eV}$  and an estimated HOMO energy of  $-5.2 \text{ eV}$  according to  $E_{\text{HOMO}} = E_{\text{LUMO}} - E_g^{\text{film}}$ ,<sup>23</sup> while PNDI-DPP (with DPP and NDI units) shows both a LUMO ( $-3.93 \text{ eV}$ ) and HOMO ( $-5.45 \text{ eV}$ ) in our measurement [Supporting Information Fig. S2(b)].<sup>20</sup> Cyclic voltammetry reveals that the new polymer PDPP2T-BT-*co*-NDI has a LUMO of  $-4.28 \text{ eV}$  and HOMO of  $-5.49 \text{ eV}$  [Supporting Information Fig. S2(a)], meaning that the HOMO and LUMO of the new polymer are even deeper than that of the PNDI-DPP copolymer. The LUMO and HOMO levels of PDPP2T-BT-*co*-DTP are rather well tuned for electron and hole injection in OFETs since Au, which is used as an electrode, has a work function of  $-5.0 \text{ eV}$ .

The polymer was first tested in thin film OFETs with a bottom contact configuration using a Si/SiO<sub>2</sub> substrate containing strip gold electrodes. Thin polymer films were deposited by spin coating and thermally annealed in vacuum ( $10^{-3} \text{ Pa}$ ) at different temperatures (120–180 °C) to optimize device performance. The hole and electron mobilities as function of the annealing temperatures and measurement conditions (inert atmosphere and air) are summarized in Supporting Information Table S1. Optimized hole and electron mobilities were achieved by annealing at 160 °C and 140 °C, and were  $4.8 \times 10^{-2}$  and  $1.2 \times 10^{-2} \text{ cm}^2 \text{ V}^{-1} \text{ s}^{-1}$ , respectively when measured in inert atmosphere (Fig. 3 and Table 1). These values slightly dropped to  $1.6 \times 10^{-2}$  and  $5.7 \times 10^{-3} \text{ cm}^2 \text{ V}^{-1} \text{ s}^{-1}$  when measured in air (Supporting Information Fig. S3 and Table 1). The hole and electron mobilities are also comparable to those of other DPP polymers, when using the same device configuration.<sup>24</sup>

**TABLE 1** Optimized Hole and Electron Mobility in Field-Effect Transistors of PDPP2T-BT-*co*-NDI Thin Films and Nanowires (NW) Measured in Inert Atmosphere or Air

		$\mu_h$ ( $\text{cm}^2 \text{V}^{-1} \text{s}^{-1}$ )	$\mu_e$ ( $\text{cm}^2 \text{V}^{-1} \text{s}^{-1}$ )
Thin film	Inert	$4.8 \times 10^{-2}$	$1.2 \times 10^{-2}$
Thin film	Air	$1.6 \times 10^{-2}$	$5.7 \times 10^{-3}$
NW	Inert	1.61	0.98
NW	Air	1.64	0.14

The new polymer showed good crystallinity as indicated by the X-ray diffraction (XRD) measurement (Supporting Information Fig. S4). This prompted us to try to further improve charge mobility by fabricating polymer nanowires. It has been reported that polymer nanowire devices exhibit significantly enhanced charge transport properties due to the high long-range order of the polymer packing.<sup>25–30</sup> In this work, PDPP2T-BT-*co*-NDI nanowires were grown on the substrate from a dilute  $\text{CHCl}_3$  solution ( $0.01 \text{ mg mL}^{-1}$ ) in a closed container, saturated with  $\text{CHCl}_3$  vapor.<sup>31</sup> As shown by optical microscopy (Supporting Information Fig. S5), atomic force microscopy (AFM) (Supporting Information Fig. S6), and scanning electron microscopy (SEM) [Fig. 4(a)], the polymer nanowires shows excellent long range regularity with a length  $> 50 \mu\text{m}$ , a width of around  $0.8 \mu\text{m}$ , and a thickness of around  $85 \text{ nm}$ .

To determine the molecular arrangement within the polymer nanowires, they were further analyzed by in transmission electron microscopy (TEM), selected area electron diffraction (SAED), and XRD [Fig. 4(b,c)]. The SAED pattern [Fig. 4(b)] exhibits several regularly spaced diffraction spots indicating that, at least locally, the nanowire is a single crystal. The reflections along the fiber direction  $[001]$  represent a  $d$ -spacing of  $5.13 \text{ \AA}$ , while those perpendicular to the

fiber direction  $[010]$  correspond to  $2.81 \text{ \AA}$ . XRD was also used to study the out of plane diffraction of the polymer nanowire [Fig. 4(c)]. The XRD shows only one sharp peak with a  $d$ -spacing of  $6.28 \text{ \AA}$ . We have not been able to unambiguously assign these spots to specific  $(hkl)$  reflections, and note that the crystal lattice parameters of the nanowire can be multiples of the distances mentioned. From density functional theory calculations, we estimate the length of the polymer repeat unit to be  $36.8 \text{ \AA}$  (Supporting Information Fig. S7). Interestingly, the crystal lattice parameters of the nanowires differ from those obtained from the XRD measurement on thermally annealed polymer films. The XRD measurements on the polymer thin films show a clear diffraction peak at  $20.8^\circ$ , which we assign to the lamellar spacing, and a reflection corresponding to  $4.0 \text{ \AA}$ , typical for  $\pi$ - $\pi$  stacking (Supporting Information Fig. S4). The absence of a correlation between the crystal lattice parameters of the nanowires and the thermally annealed thin films suggests that these two have different crystal structures. The apparent polymorphism might originate from the different preparation conditions.

OFETs based on a polymer nanowire were constructed using a bottom gate—top contact configuration, where the polymer nanowire was grown on top of an octadecyltrichlorosilane (OTS)—modified  $\text{Si/SiO}_2$  substrate. Au source and drain electrodes were deposited on the nanowire by thermal evaporation with an organic ribbon as the mask (Supporting Information Fig. S8).<sup>32</sup> The transistors based on the polymer nanowire exhibit ambipolar charge transport with hole and electron mobilities of  $1.61$  and  $0.98 \text{ cm}^2 \text{V}^{-1} \text{s}^{-1}$  (Fig. 5 and Table 1) in inert atmosphere. When measured in air, the hole mobility remains almost constant ( $1.64 \text{ cm}^2 \text{V}^{-1} \text{s}^{-1}$ ), but electron mobility is slightly decreased to  $0.14 \text{ cm}^2 \text{V}^{-1} \text{s}^{-1}$  (Supporting Information Fig. S9). The decreased electron mobility in ambient air is attributed to the effect of the

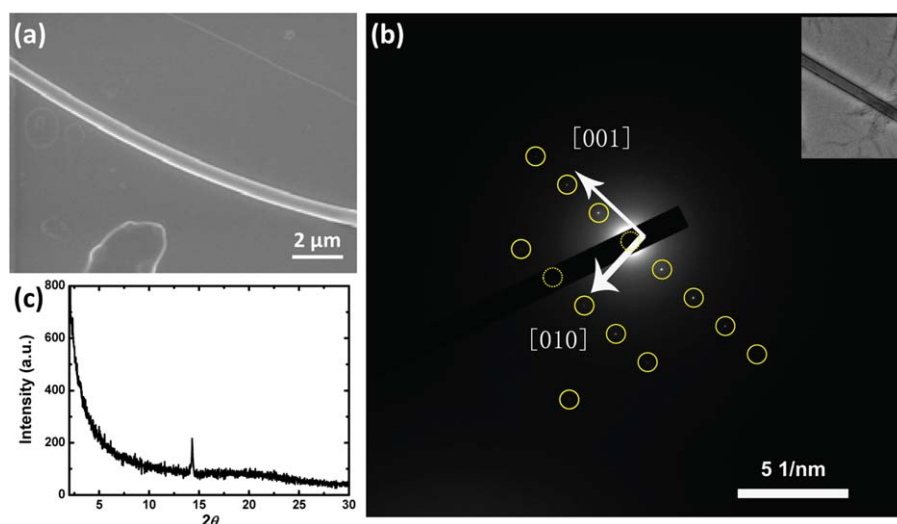


**FIGURE 4** (a) SEM image, (b) SAED pattern, and (c) out-of-plane X-ray diffraction patterns of a PDPP2T-BT-*co*-NDI single nanowire. TEM image is shown in the insert of (b). The solid circles in panel (b) are a guide to the eye to identify observable reflections. [Color figure can be viewed in the online issue, which is available at [wileyonlinelibrary.com](http://www.wileyonlinelibrary.com).]

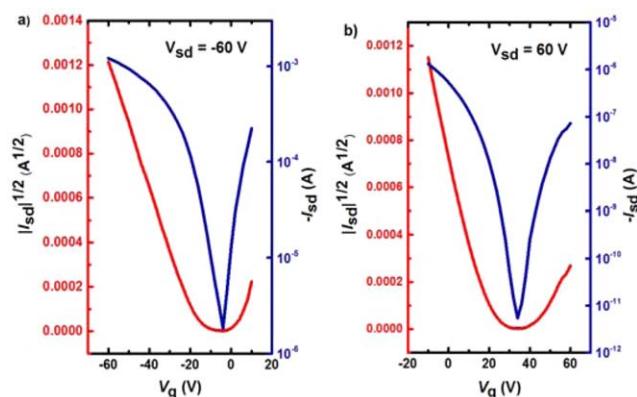


**FIGURE 5** (a) p-type and (b) n-type transfer characteristics for PDPP2T-BT-co-NDI nanowires based OFETs with top contact configuration measured under inert atmosphere. [Color figure can be viewed in the online issue, which is available at [wileyonlinelibrary.com](http://wileyonlinelibrary.com).]

exposure of the polymer nanowire to water and oxygen.<sup>33,34</sup> The new polymer PDPP2T-BT-co-NDI has an estimated LUMO level of  $-4.28$  eV, which is close to value of  $-4.0$  to  $-4.1$  eV, previously reported as the threshold for electron stabilization during charge transport.<sup>33</sup> This may explain the decreased electron mobility in both thin films and polymer nanowires.

In conclusion, in this work a new polymer, PDPP2T-BT-co-NDI, with ternary electron-deficient units was designed for use in ambipolar OFETs. The polymer showed hole and electron mobilities of  $4.8 \times 10^{-2}$  and  $1.2 \times 10^{-2} \text{ cm}^2 \text{ V}^{-1} \text{ s}^{-1}$  in thin film OFETs and  $1.61$  and  $0.98 \text{ cm}^2 \text{ V}^{-1} \text{ s}^{-1}$  in nanowire OFETs. Hole and electron mobilities measured in ambient air were still as high as  $1.64$  and  $0.14 \text{ cm}^2 \text{ V}^{-1} \text{ s}^{-1}$ . The results demonstrate that introduction of multi-electron-deficient units into one conjugated polymer is an efficient way to tune the energy level and realize high performance ambipolar OFETs.

## ACKNOWLEDGMENTS

Authors thank Ralf Bovee at Eindhoven University of Technology (TU/e, Netherlands) for GPC analysis. This work was supported by the Recruitment Program of Global Youth Experts of China. The work was further supported by the Ministry of Science and Technology of China (2014CB643600, 2013CB933500), the National Natural Science Foundation of China (21474026) and the Strategic Priority Research Program (Grant No. XDB12030300) of the Chinese Academy of Sciences. The research forms part of the Solliance OPV programme and has received funding from the Ministry of Education, Culture and Science (Gravity program 024.001.035) of the Netherlands.

## REFERENCES AND NOTES

1 H. Sirringhaus, *Adv. Mater.* **2014**, *26*, 1319–1335.

- 2 J. Y. Back, H. Yu, I. Song, I. Kang, H. Ahn, T. J. Shin, S. K. Kwon, J. H. Oh, Y. H. Kim, *Chem. Mater.* **2015**, *27*, 1732–1739.
- 3 B. Sun, W. Hong, Z. Yan, H. Aziz, Y. Li, *Adv. Mater.* **2014**, *26*, 2636–2642.
- 4 Y. Zhao, Y. Guo, Y. Liu, *Adv. Mater.* **2013**, *25*, 5372–5391.
- 5 J. Lee, A. Han, H. Yu, T. Shin, C. Yang, J. Oh, *J. Am. Chem. Soc.* **2013**, *135*, 9540–9547.
- 6 B. Sun, W. Hong, H. Aziz, Y. Li, *Polym. Chem.* **2015**, *6*, 938–945.
- 7 F. S. Kim, X. Guo, M. D. Watson, S. A. Jenekhe, *Adv. Mater.* **2010**, *22*, 478–482.
- 8 R. Capelli, S. Toffanin, G. Generali, H. Usta, A. Facchetti, M. Muccini, *Nat. Mater.* **2010**, *9*, 496–503.
- 9 J. Zaumseil, H. Sirringhaus, *Chem. Rev.* **2007**, *107*, 1296–1323.
- 10 Y. J. Cheng, S. H. Yang, C. S. Hsu, *Chem. Rev.* **2009**, *109*, 5868–5923.
- 11 K. H. Hendriks, W. Li, M. M. Wienk, R. A. J. Janssen, *J. Am. Chem. Soc.* **2014**, *136*, 12130–12136.
- 12 J. K. Lee, M. C. Gwinner, R. Berger, C. Newby, R. Zentel, R. H. Friend, H. Sirringhaus, C. K. Ober, *J. Am. Chem. Soc.* **2011**, *133*, 9949–9951.
- 13 G. Kim, A. R. Han, H. R. Lee, J. Lee, J. H. Oh, C. Yang, *Chem. Commun.* **2014**, *50*, 2180–2183.
- 14 C. W. Ge, C. Y. Mei, J. Ling, J. T. Wang, F. G. Zhao, L. Liang, H. J. Li, Y. S. Xie, W. S. Li, *J. Polym. Sci. Part A: Polym. Chem.* **2014**, *52*, 1200–1215.
- 15 F. Grenier, P. Berrouard, J. R. Pouliot, H. R. Tseng, A. J. Heeger, M. Leclerc, *Polym. Chem.* **2013**, *4*, 1836–1841.
- 16 R. S. Ashraf, A. J. Kronemeijer, D. I. James, H. Sirringhaus, I. McCulloch, *Chem. Commun.* **2012**, *48*, 3939–3941.
- 17 J. D. Yuen, J. Fan, J. Seifter, B. Lim, R. Hufschmid, A. J. Heeger, F. Wudl, *J. Am. Chem. Soc.* **2011**, *133*, 20799–20807.
- 18 P. Wang, H. Li, C. Gu, H. Dong, Z. Xu, H. Fu, *RSC Adv.* **2015**, *5*, 19520–19527.
- 19 P. Sonar, S. P. Singh, Y. Li, M. S. Soh, A. Dodabalapur, *Adv. Mater.* **2010**, *22*, 5409–5413.
- 20 X. Guo, A. Facchetti, T. J. Marks, *Chem. Rev.* **2014**, *114*, 8943–9021.
- 21 Z. Chen, Y. Zheng, H. Yan, A. Facchetti, *J. Am. Chem. Soc.* **2009**, *131*, 8–9.
- 22 W. Li, K. H. Hendriks, A. Furlan, W. S. C. Roelofs, M. M. Wienk, R. A. J. Janssen, *J. Am. Chem. Soc.* **2013**, *135*, 18942–18948.
- 23 W. Li, K. H. Hendriks, A. Furlan, A. Zhang, M. M. Wienk, R. A. J. Janssen, *Chem. Commun.* **2015**, *51*, 4290–4293.
- 24 W. Li, W. S. C. Roelofs, M. M. Wienk, R. A. J. Janssen, *J. Am. Chem. Soc.* **2012**, *134*, 13787–13795.
- 25 J. H. Kim, D. H. Lee, D. S. Yang, D. U. Heo, K. H. Kim, J. Shin, H. J. Kim, K. Y. Baek, K. Lee, H. Baik, M. J. Cho, D. H. Choi, *Adv. Mater.* **2013**, *25*, 4102–4106.
- 26 S. H. Wang, M. Kappl, I. Liebewirth, M. Muller, K. Kirchhoff, W. Pisula, K. Mullen, *Adv. Mater.* **2012**, *24*, 417–420.
- 27 A. L. Briseno, S. C. B. Mannsfeld, X. Lu, Y. Xiong, S. A. Jenekhe, Z. Bao, Y. Xia, *Nano Lett.* **2007**, *7*, 668–675.
- 28 H. Xin, G. Ren, F. S. Kim, S. A. Jenekhe, *Chem. Mater.* **2008**, *20*, 6199–6207.
- 29 F. Li, K. G. Yager, N. M. Dawson, Y. B. Jiang, K. J. Malloy, Y. Qin, *Chem. Mater.* **2014**, *26*, 3747–3756.
- 30 F. Li, K. G. Yager, N. M. Dawson, Y. B. Jiang, K. J. Malloy, Y. Qin, *Polym. Chem.* **2015**, *6*, 721–731.



**31** H. Dong, S. Jiang, L. Jiang, Y. Liu, H. Li, W. Hu, E. Wang, S. Yan, Z. Wei, W. Xu, X. Gong, *J. Am. Chem. Soc.* **2009**, *131*, 17315–17320.

**32** L. Jiang, J. Gao, E. Wang, H. Li, Z. Wang, W. Hu, L. Jiang, *Adv. Mater.* **2008**, *20*, 2735–2740.

**33** H. Usta, C. Risko, Z. Wang, H. Huang, M. K. Deliomeroğlu, A. Zhukhovitskiy, A. Facchetti, T. J. Marks, *J. Am. Chem. Soc.* **2009**, *131*, 5586–5608.

**34** B. A. Jones, A. Facchetti, M. R. Wasielewski, T. J. Marks, *J. Am. Chem. Soc.* **2007**, *129*, 15259–15278.